MUCOSAL IMMUNOLOGY

IL-1R1–dependent signaling coordinates epithelial regeneration in response to intestinal damage

Christian B. Cox[1†], Elaine E. Storm[2†], Varun N. Kapoor[3], Joseph Chavarria-Smith[1], David L. Lin[1], Lifen Wang[1], Yun Li[1], Noelyn Kljavin[2], Naruhisa Ota[1], Travis W. Bainbridge[4], Keith Anderson[5], Merone Roose-Girma[5], Søren Warming[5], Joseph R. Arron[1], Shannon J. Turley[3], Frederic J. de Sauvage[2]*, Menno van Lookeren Campagne[1]*‡

Repair of the intestinal epithelium is tightly regulated to maintain homeostasis. The response after epithelial damage needs to be local and proportional to the insult. How different types of damage are coupled to repair remains incompletely understood. We report that after distinct types of intestinal epithelial damage, IL-1R1 signaling in GREM1$^+$ mesenchymal cells increases production of R-spondin 3 (RSPO3), a Wnt agonist required for intestinal stem cell self-renewal. In parallel, IL-1R1 signaling regulates IL-22 production by innate lymphoid cells and promotes epithelial hyperplasia and regeneration. Although the regulation of both RSPO3 and IL-22 is critical for epithelial recovery from *Citrobacter rodentium* infection, IL-1R1–dependent RSPO3 production by GREM1$^+$ mesenchymal cells alone is sufficient and required for recovery after dextran sulfate sodium–induced colitis. These data demonstrate how IL-1R1–dependent signaling orchestrates distinct repair programs tailored to the type of injury sustained that are required to restore intestinal epithelial barrier function.

INTRODUCTION

Adult intestinal stem cells (ISCs) sustain tissue function throughout life, regulating homeostasis and regeneration after injury. ISCs are characterized by their ability to asymmetrically divide: self-renewing to maintain their own pool and producing progeny that can differentiate into multiple epithelial cell types (*1*). The ratio of self-renewal to differentiation in proliferating ISCs is critical for proper tissue function and is tightly regulated in the intestine through gradients of stem cell niche factors (*2*–*5*). In the small intestine, the stem cell niche is composed of epithelial Paneth cells and of mesenchymal cells (*6*). However, the colon lacks Paneth cells, and as a result, the ISCs are more dependent on mesenchymal factors (*7*–*10*).

Most of the epithelial cells in the intestine turn over once every 5 days, driven by a highly proliferative progenitor compartment that can regenerate the epithelium after damage through WNT-dependent and WNT-independent processes (*11*, *12*). Peri-cryptal mesenchymal cells have been identified as a potential source of trophic factors that support epithelial restitution (*6*, *7*, *9*, *10*, *12*–*15*). In response to epithelial injury by mechanical stress, infection, cytotoxic therapies, and chronic inflammation, epithelial renewal needs to be accelerated to maintain epithelial barrier function. Our understanding of how inflammation affects these mesenchymal subsets to stimulate stem cell self-renewal and improve epithelial barrier function after injury remains incomplete. Because mucosal healing is required for achieving long-term remission in inflammatory bowel disease (IBD) (*16*), identifying the impact of inflammatory mediators, such as cytokines, on epithelial barrier function will be critical.

[1]Department of Immunology, Genentech Inc., South San Francisco, CA 94080, USA. [2]Department of Molecular Oncology, Genentech Inc., South San Francisco, CA 94080, USA. [3]Department of Cancer Immunology, Genentech Inc., South San Francisco, CA 94080, USA. [4]Department of Protein Chemistry, Genentech Inc., South San Francisco, CA 94080, USA. [5]Department of Molecular Biology, Genentech Inc., South San Francisco, CA 94080, USA.
*Corresponding author. Email: desauvage.fred@gene.com (F.J.d.S.); mennocampagne@gmail.com (M.v.L.C.)
†These authors contributed equally to this work.
‡Present address: Department of Inflammation and Oncology, Amgen Research, Amgen Inc., South San Francisco, CA 94080, USA.

Interleukin-1 (IL-1) cytokines IL-1α and IL-1β are released after pathogen infection or damage to the colon and have been implicated in epithelial repair (*17*–*19*). IL-1R1 is a shared receptor for IL-1α and IL-1β and is expressed on multiple cell types in the colon (*20*). To test our hypothesis that IL-1R1 signaling may be an important integrator of injury-specific pathways required for colonic epithelial repair, we conditionally deleted IL-1R1 in specific mesenchymal cell types to examine the effects on the epithelium after pathogen- and chemical-induced damage in the colon.

RESULTS

IL-1R1 is required for renewal of *Lgr5*$^+$ stem cells after *Citrobacter rodentium* infection

C. rodentium is an attaching/effacing bacterium that infects epithelial cells, resulting in epithelial hyperplasia and transient diarrhea (*21*). Mice that lack IL-1R1 are highly susceptible to *C. rodentium* (Fig. 1A and fig. S1A) (*22*). Both *Il1α* and *Il1β* were up-regulated in the colon in response to *C. rodentium* (Fig. 1B). In addition, *Cxcl1*, *Il18*, *Il33*, *Il6*, and *Il17a* were induced by *C. rodentium* (fig. S1B) with *Il1α*, *Il6*, and *Il17a* showing IL-1R1–dependent regulation, consistent with previous reports (*23*, *24*). To evaluate the relative contribution of IL-1α and IL-1β, we used blocking antibodies and *Caspase 1/11* double knockout (KO) mice (*25*). Antibodies against IL-1α showed a greater increase in susceptibility to *C. rodentium* compared with IL-1β–neutralizing antibodies (fig. S2A). A minor increase in susceptibility to *C. rodentium* infection after IL-1β blockade was consistent with similar results obtained in *Caspase 1/11* double KO mice that are unable to process IL-1β to its active form (fig. S2B).

To determine how IL-1R1 signaling protects against *C. rodentium*, we examined histology and gene expression in the distal colon at various time points after infection. We observed that susceptibility was associated with loss of crypt density and integrity of the epithelial barrier, with *Il1r1* KO mice having significantly lower crypt density throughout the colon at days 7 and 11 after infection (Fig. 1, C and D). Consistent with a reduction in crypt density, markers of ISCs were also affected. In *Il1r1* HET mice, the Wnt target genes *Lgr5* and

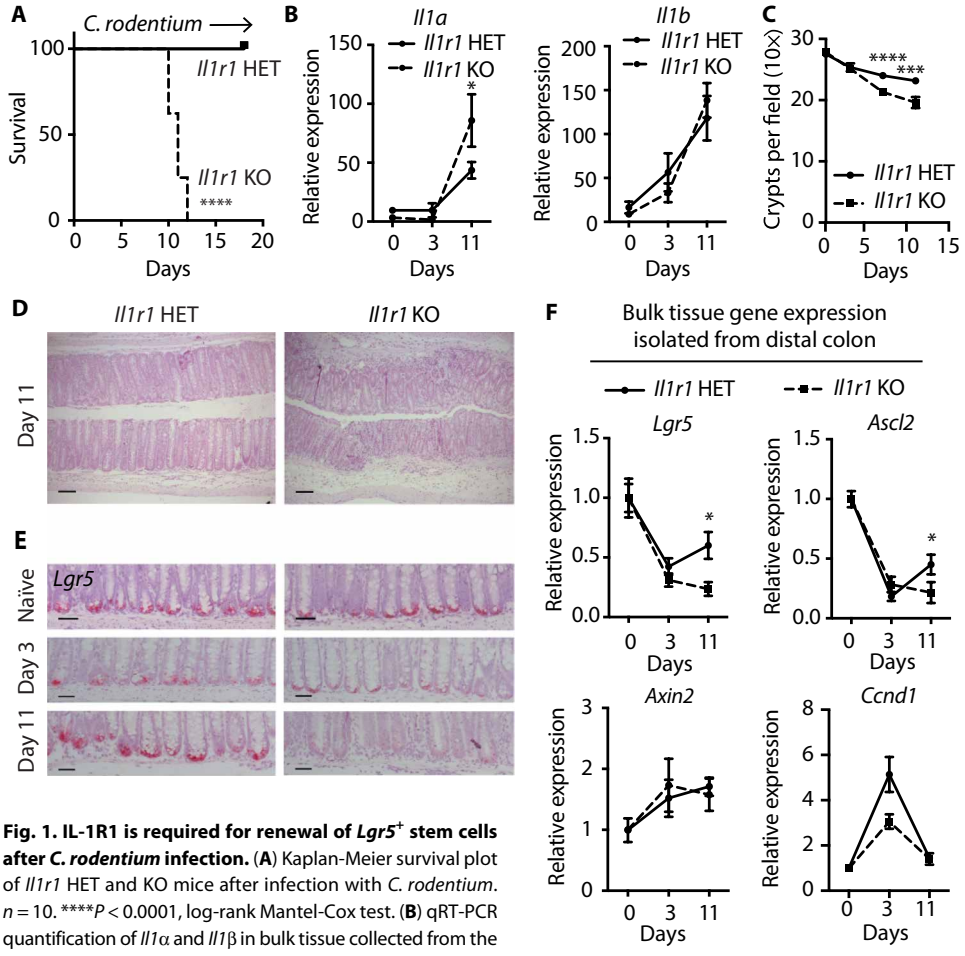

Fig. 1. IL-1R1 is required for renewal of *Lgr5*$^+$ stem cells after *C. rodentium* infection. (**A**) Kaplan-Meier survival plot of *Il1r1* HET and KO mice after infection with *C. rodentium*. $n = 10$. ****$P < 0.0001$, log-rank Mantel-Cox test. (**B**) qRT-PCR quantification of *Il1α* and *Il1β* in bulk tissue collected from the colon at various time points during infection with *C. rodentium*. $n = 4$, *$P < 0.05$, Student's t test. (**C**) Quantification of crypt density in a 1500-μm segment of the colon. $n = 10$, ***$P < 0.005$ and ****$P < 0.0001$. Multiple t test. (**D**) H&E-stained section of the colon of *Il1r1* HET and KO mice 11 days after infection with *C. rodentium*. Scale bars, 100 μm. (**E**) ISH of *Lgr5* in the colon of naïve mice and 3 and 11 days after *C. rodentium* infection. Scale bars, 50 μm. (**F**) qRT-PCR gene expression of *Lgr5*, *Ascl2*, *Axin2*, and *Ccnd1* in bulk tissue collected from the distal colon in *Il1r1* HET and KO mice at baseline and days 3 and 11 after infection with *C. rodentium*. $n = 4$, *$P < 0.05$. Multiple t test. Error bars in (B), (C), and (F) indicate SEM. All experiments were repeated at least twice with similar results.

Ascl2 were initially reduced after infection but began to normalize by day 11. This normalization of stem cell gene expression was not apparent in *Il1r1* KO mice, which showed continued reduced stem cell gene expression at day 11 (Fig. 1, E and F). The effect of *Il1r1* KO on *Ascl2* and *Lgr5* was not accompanied by a reduction in classical Wnt target genes such as *Axin2* or *Ccnd1*, which are expressed in both stem cells and transit amplifying cells (*26*), suggesting that IL-1 supports epithelial repair primarily by promoting Wnt target gene expression specific to ISCs.

IL-1R1–dependent induction of R-spondin 3 in stromal cells is required for *Lgr5*$^+$ stem cell renewal and epithelial barrier repair after *C. rodentium* infection

To narrow down the cell types in which IL-1R1 signaling is required for resistance to *C. rodentium* infection, we adoptively transferred *Il1r1* wild-type (WT) or KO bone marrow–derived cells into *Il1r1* WT or KO irradiated recipient hosts. Using this approach, we found that IL-1R1 signaling in radiation-resistant cells was required to protect the host from *C. rodentium* infection (Fig. 2A). Whereas the IL-1 decoy receptor *Il1r2* was predominantly expressed on gut epithelial cells, *Il1r1* expression levels were enriched more than 10-fold in nonepithelial cells (Fig. 2B). These data suggest that nonepithelial, radiation-resistant stromal cells are an important source of IL-1R1 signaling, consistent with the transcriptional response observed in these cells in vitro after stimulation with IL-1α and IL-1β (fig. S2C).

Because stromal cells have been identified as a major component of the stem cell niche in the colon, we determined whether IL-1R1–dependent signaling induced candidate stem cell niche factors in stromal cells derived from the mouse colon. IL-1α and IL-1β did not affect Wnt ligand production, which is consistent with the lack of reduction in general Wnt target genes observed in *Il1r1* KO mice, but strongly up-regulated expression of *Rspo3*, a Wnt signal amplifier required for *Lgr5* expression and intestinal regeneration (Fig. 2C) (*27*, *28*). Consistent with these in vitro results, IL-1R1 signaling was required for increased *Rspo3* expression in the colon in response to *C. rodentium* infection (Fig. 2D). In an in vitro coculture system of primary colonic mesenchymal cells with colonic epithelial organoids, we found that IL-1α– and IL-1β–induced signaling in mesenchymal cells was sufficient to maintain *Lgr5* transcription in the organoids in the absence of any exogenously supplied factors (Fig. 2E). This phenotype was dependent on R-spondin 3 (RSPO3), as antibody neutralization of RSPO3 blocked the ability of IL-1α or IL-1β to increase *Lgr5* mRNA expression in organoids (Fig. 2F) (*28*). *Il1r1* HET mice treated with neutralizing anti-RSPO3 antibodies were highly susceptible to *C. rodentium* infection, which was associated with a significant decrease in *Lgr5* expression (Fig. 2G). Blocking RSPO3 in *Il1r1* KO mice further impaired resistance compared with their *Il1r1* HET littermates, indicating that RSPO3 production is not dependent on IL-1R1 activation alone. In turn, administration of recombinant RSPO3 increased *Lgr5* expression and crypt density and rescued *Il1r1* KO mice (Fig. 2H and fig. S3, A to C). These data indicate that IL-1 regulation of RSPO3 production by mesenchymal cells maintains the ISC compartment and plays a critical role in host defense against *C. rodentium*.

IL-1R1 induces *Rspo3* expression in a unique population of *Grem1*$^+$ mesenchymal cells

Because mesenchymal cells within the intestine consist of a heterogeneous population of cells (*15*), we set out to define which subpopulation of mesenchymal cells shows IL-1R1–dependent induction of

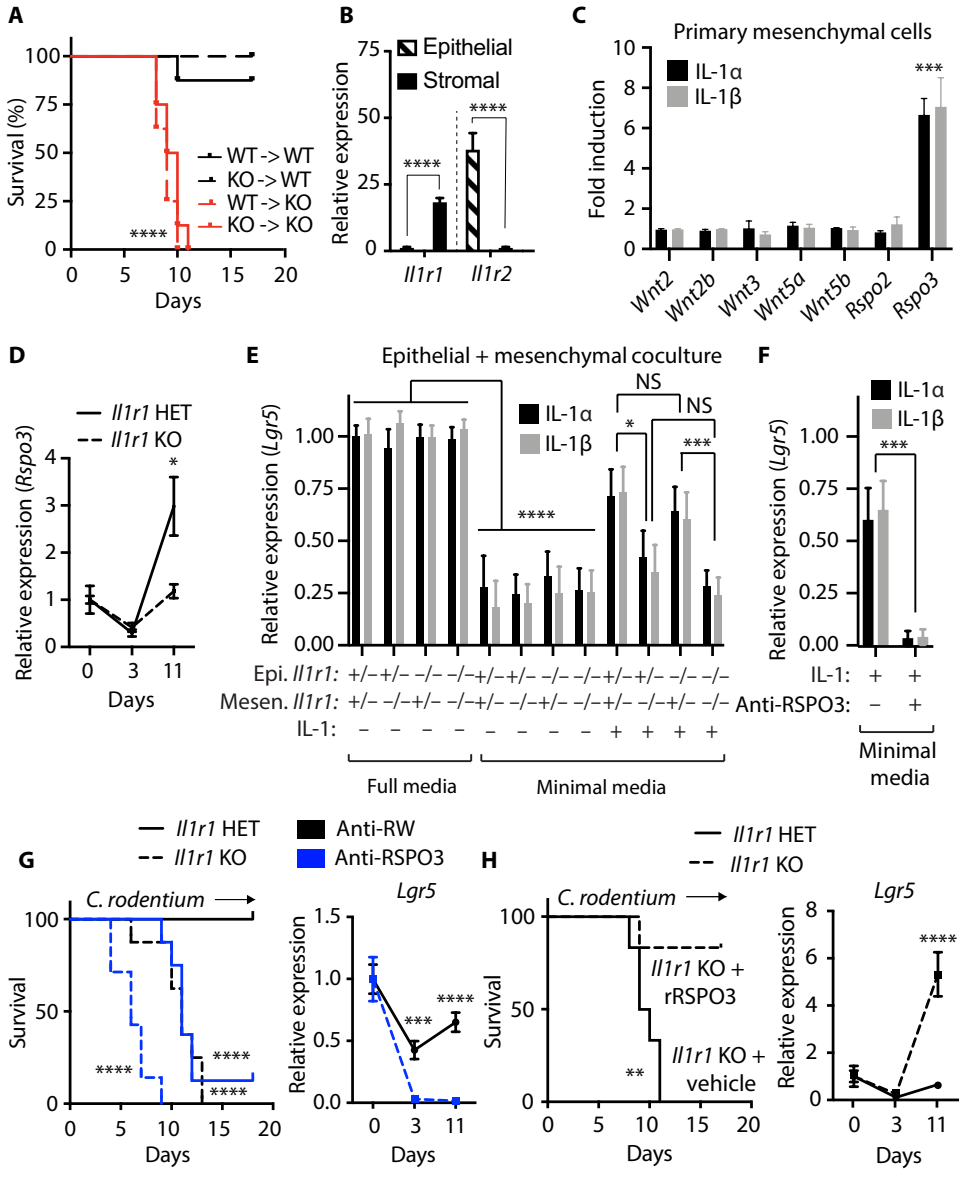

Fig. 2. IL-1R1–dependent induction of RSPO3 in stromal cells is required for *Lgr5*$^+$ stem cell renewal and epithelial barrier repair after *C. rodentium* infection. (**A**) Kaplan-Meier survival curves of *Il1r1* WT and KO bone marrow chimeras. $n = 8$, $^{****}P < 0.001$, log-rank Mantel-Cox test. (**B**) qRT-PCR gene expression of *Il1r1* and *Il1r2* in epithelial and stromal cells isolated from the colon of naïve mice. $n = 5$, $^{****}P < 0.001$. Student's *t* test. (**C**) Expression of *Wnt* and *R-spondin* ligands in primary colonic stromal cells stimulated with 1 ng/ml of IL-1α or IL-1β for 24 hours. *Gapdh* was used as a housekeeping gene to normalize expression data. Data are expressed in fold change from unstimulated control cells. $n = 3$. $^{***}P < 0.005$, one-way ANOVA with Tukey's multiple comparisons test. (**D**) Expression of *Rspo3* in bulk tissue collected from the distal colon at indicated time points after *C. rodentium* infection. $n = 4$, $^{*}P < 0.05$, Student's *t* test. (**E**) qRT-PCR of *Lgr5* in cocultures of primary epithelial organoids and stromal cells both collected from the colon. Genotypes of epithelial organoids and primary stromal cells are indicated, and cocultures were stimulated with IL-1α or IL-1β for 48 hours. $n = 4$. $^{*}P < 0.05$, $^{***}P < 0.005$, and $^{****}P < 0.001$, one-way ANOVA with Tukey's multiple comparisons test. Epi., epithelial; Mesen., mesenchymal; Full media, full stem cell media. (**F**) qRT-PCR of *Lgr5* expression in cocultures stimulated with IL-1α or IL-1β for 48 hours and treated with vehicle or RSPO3-neutralizing antibody. $n = 4$, $^{***}P < 0.005$, Student's *t* test. (**G**) Kaplan-Meier survival curve for *Il1r1* HET and KO mice treated with a control antibody or a RSPO3-neutralizing antibody after infection with *C. rodentium*. $n = 8$, $^{****}P < 0.001$, log-rank Mantel-Cox test. Right: *Lgr5* expression by qRT-PCR in bulk colonic tissue from *Il1r1* WT mice. $n = 4$, $^{***}P < 0.005$ and $^{****}P < 0.001$, Student's *t* test. (**H**) Survival of *Il1r1* KO mice treated with vehicle or recombinant RSPO3 after infection with *C. rodentium*. $n = 8$, $^{**}P < 0.01$, log-rank Mantel-Cox test. Right: *Lgr5* expression by qRT-PCR in bulk colonic tissue from mice in a similar experiment. $n = 4$, $^{****}P < 0.001$, Student's *t* test. Error bars in (B) to (H) indicate SEM. Experiments were repeated at least twice with similar results. NS, not significant.

Rspo3. Using in situ hybridization (ISH), we found that *Rspo3* is predominantly expressed in the muscularis mucosae and is visibly increased at day 11 after *C. rodentium* infection (fig. S4A). To further define this population of cells, we performed dual ISH with known mesenchymal markers. *Col1a1* expression was found expressed in subepithelial mesenchymal cells along the crypt and coexpressed with *Rspo3* in the muscularis mucosae (Fig. 3A). *Pdgfra* expression was found primarily in subepithelial mesenchymal cells along the crypt and was not strongly coexpressed with *Rspo3* in the muscularis mucosae (Fig. 3B). In contrast, *Grem1*, marking a population of cells (trophocytes) required for *Lgr5* expression in the small intestine (*29*), was coexpressed with *Rspo3* (Fig. 3C). Other mesenchymal cell markers including *Cd34*, *Gli1*, and *Foxl1* were minimally coexpressed with *Rspo3* (fig. S4B). Isolated primary GREM1$^+$, PDGFRA^{hi}, and PDGFRA^{lo} cells from the colon confirmed that *Rspo3* is enriched in GREM1$^+$ cells, whereas *Wnt4* is enriched in PDGFRA^{hi} cells (Fig. 3D). ISH of *Grem1* and *Pdgfra* also confirmed that these cell markers are minimally coexpressed (fig. S5, A to D). *Il1r1* was expressed in PDGFRA^{hi}, PDGFRA^{lo}, and GREM1$^+$ cells and was increased in each cell type after infection with *C. rodentium* (Fig. 3E). We then analyzed *RSPO3*, *IL1R1*, *WNT4*, *PDGFRA*, and *GREM1* expression in a publicly available dataset of control and ulcerative colitis diagnosed human colonic biopsy samples (*15*). Matching the murine data, *GREM1* represented a unique cluster of cells that was distinct from *PDGFRA*$^+$ mesenchymal cells and that constituted the main source of *RSPO3* (fig. S6, A and B). *RSPO3*$^+$ *IL1R1*$^+$ double-positive cells formed a subset of cells within this cluster in samples from healthy controls and patients diagnosed with ulcerative colitis.

IL-1R1–dependent induction of RSPO3 in GREM1$^+$ cells is required for crypt protection after *C. rodentium* infection

Because *Il1r1* is expressed on multiple subsets of mesenchymal cells, we used three different Cre-expressing mouse lines to target *Il1r1* in mesenchymal cell populations: *Col1a1*.creERT2, *Grem1*.creERT2, and *Pdgfra*.Cre (figs. S7 and

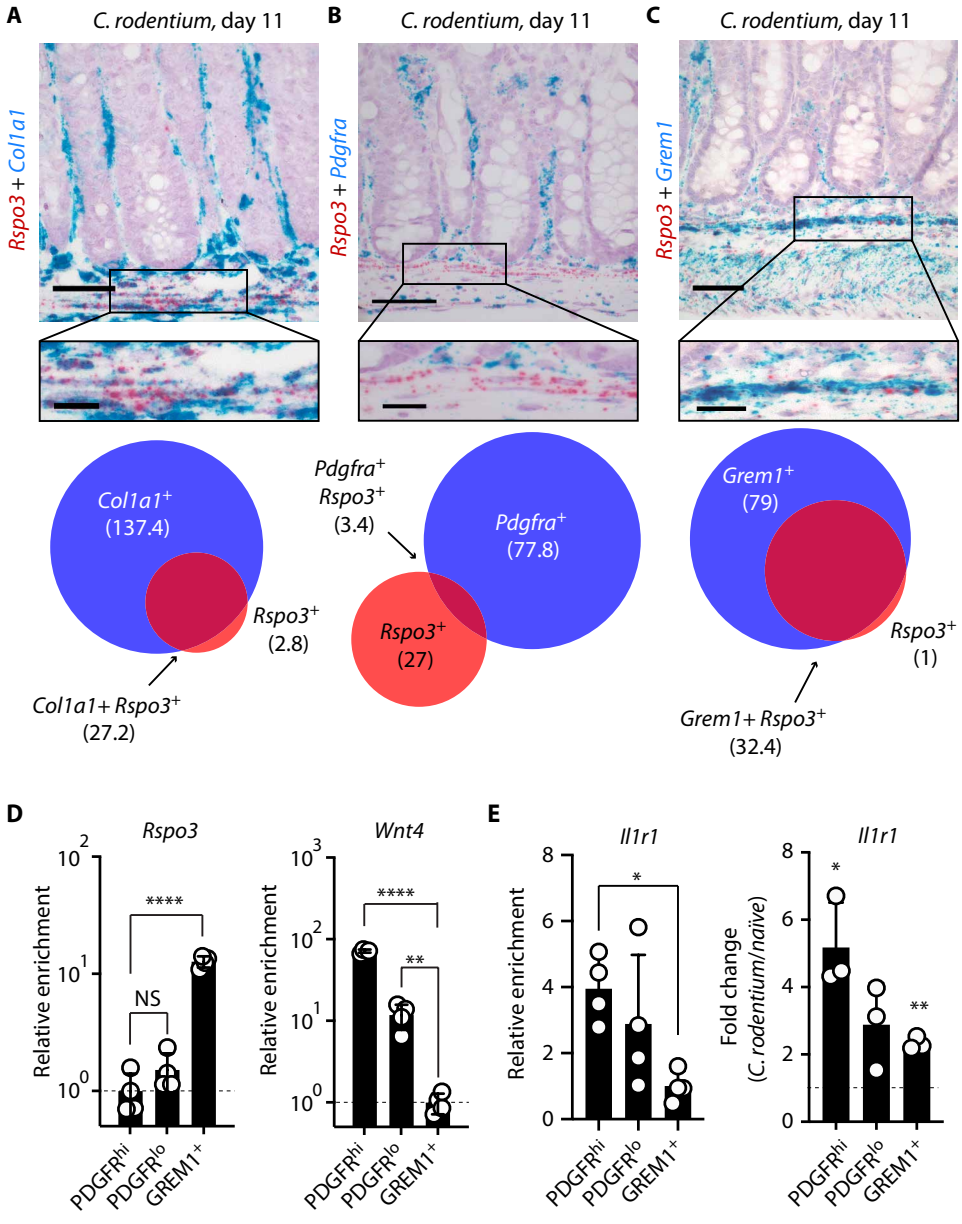

Fig. 3. Expression of *Rspo3* in GREM1$^+$ cells after *C. rodentium* infection. (**A** to **C**) Dual ISH and number of single- or dual-positive cells per square micrometer of *Rspo3* and either *Col1a1* (A), *Pdgfra* (B), or *Grem1* (C) (blue) on day 11 after infection with *C. rodentium*. Scale bars, 50 μm. (**D**) qRT-PCR gene expression of *Rspo3* and *Wnt4* in primary sorted cells. $n = 4$. $^{****}P < 0.001$ and $^{**}P < 0.01$, one-way ANOVA with Tukey's multiple comparisons test. (**E**) Left: qRT-PCR gene expression of *Il1r1* in primary sorted cells at baseline. $n = 3$. $^{**}P < 0.01$ and $^{****}P < 0.001$, one-way ANOVA with Tukey's multiple comparisons test. Right: Fold change in *Il1r1* expression on day 11 after infection with *C. rodentium*. $n = 3$. $^{*}P < 0.05$ and $^{**}P < 0.01$, Student's *t* test. Error bars in (D) and (E) indicate SEM.

S8, A to E). Whereas *Grem1* and *Pdgfra* are enriched in specific mesenchymal cell types that express *Rspo3* and *Wnt* ligands, respectively, *Col1a1* is broadly expressed in all mesenchymal cells. After *C. rodentium* infection, both *Col1a1*.creERT2 *Il1r1* loxP/loxP (*Col1a1*$^{\Delta iIl1r1}$) mice and *Grem1*.creERT2 *Il1r1* loxP/loxP (*Grem1*$^{\Delta Il1r1}$) mice recapitulated the stem cell and crypt density phenotype of germline *Il1r1* KO mice (Fig. 4, A and B). Unexpectedly, *Pdgfra*.Cre *Il1r1* loxP/loxP (*Pdgfra*$^{\Delta Il1r1}$) mice did not, indicating that unlike GREM1$^+$ cells, IL-1R1–dependent signaling in Wnt ligand–expressing PDGFRα$^+$ mesenchymal cells is not required for crypt maintenance after *C. rodentium* infection. IL-1R1–dependent regulation of *Rspo3* levels during infection appears to result from both an increase in the number of expressing cells and an increase in the expression level of *Rspo3* per cell, because the percentage of GREM1$^+$ cells 11 days after infection was significantly lower in the *Grem1*$^{\Delta iIl1r1}$ mice when compared with their *Grem1*.creERT2 *Il1r1* WT/loxP (*Grem1*$^{WT/loxP}$) littermate controls after infection (fig. S9).

IL-1R1–dependent induction of IL-22 in ILCs contributes to host resistance and epithelial regeneration after *C. rodentium* infection

Despite similar effects on crypt density and *Lgr5* and *Rspo3* expression, *Col1a1*$^{\Delta iIl1r1}$ mice were more susceptible to *C. rodentium* than *Grem1*$^{\Delta iIl1r1}$ mice (Fig. 4C). This suggested that IL-1R1 signaling in COL1A1$^+$ GREM1$^-$ cells contributed to *C. rodentium* resistance. To identify these cells, we explored additional factors known to be critical for protection to this pathogen. IL-22, an essential cytokine in the response to *C. rodentium*, is known to be regulated by IL-1 (*30*, *31*). We confirmed the critical role of IL-22 in this model (Fig. 5A) and show IL-1R1–dependent regulation of *Il22* and its response gene, *Reg3g*, in the colon (Fig. 5, B and C). *Reg3g* was reduced in germline KO and *Col1a1*$^{\Delta iIl1r1}$ mice but not in *Grem1*$^{\Delta iIl1r1}$ compared with *Grem1*$^{WT/loxP}$ mice. This suggests that COL1A1$^+$ GREM1$^-$ cells are responsible for the difference in susceptibility and may be a source of IL-22. There are two known sources of IL-22 in the colon: innate lymphoid cells (ILCs) and CD4$^+$ T cells. On the basis of known requirements during the early innate phase of infection and the partial susceptibility of mice lacking T cells (*32*), ILC-derived IL-22 is thought to be critical for resistance to *C. rodentium* (*30*, *33*). Furthermore, ILCs are reported to be radioresistant (*34*). Because our bone marrow transfer experiment suggested that IL-1R signaling is required on radioresistant populations, we focused our attention on ILCs. In the *Il1r1* KO mice, IL-22$^+$ ILCs were reduced after infection with *C. rodentium* and unresponsive to exogenous IL-1β stimulation (Fig. 5D). Furthermore, we observed COL1A1 reporter activity in ILCs from *Col1a1*$^{\Delta iIl1r1}$ mice (Fig. 5D and fig. S10), consistent with low-level expression of *Col1a1* in this cell population [Fig. 5E and (*35*)].

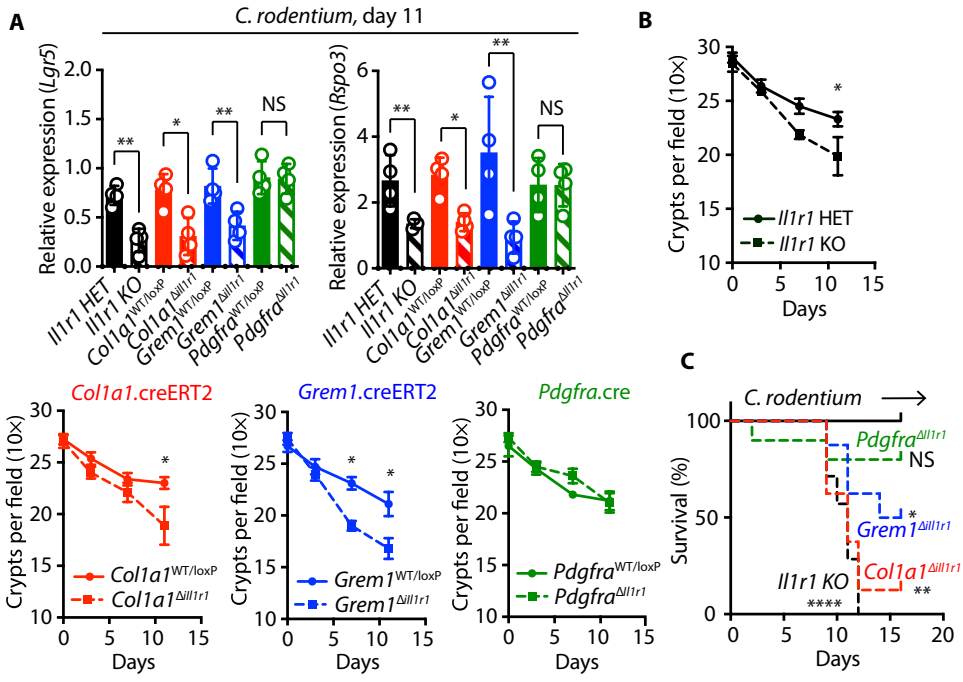

Fig. 4. IL-1R1–dependent induction of RSPO3 in GREM1$^+$ cells is required for crypt protection after *C. rodentium* infection. (**A**) qRT-PCR gene expression of *Lgr5* (left) and *Rspo3* (right) in bulk tissue collected from the distal colon of *Il1r1* HET and KO, *Col1a1*$^{\Delta il1r1}$, *Col1a1*$^{WT/loxP}$, *Grem1*$^{\Delta il1r1}$, *Grem1*$^{WT/loxP}$, *Pdgfra*$^{\Delta Il1r1}$, and *Pdgfra*$^{WT/loxP}$ mice at day 11 after infection with *C. rodentium*. $n = 4$. $^*P < 0.05$, one-way ANOVA with Tukey's multiple comparisons test. (**B**) Quantification of crypt density in 1500-μm colon segments of *Il1r1* HET and KO, *Col1a1*$^{\Delta il1r1}$, *Col1a1*$^{WT/loxP}$, *Grem1*$^{\Delta il1r1}$, *Grem1*$^{WT/loxP}$, *Pdgfra*$^{\Delta Il1r1}$, and *Pdgfra*$^{WT/loxP}$ mice at day 11 after infection with *C. rodentium*. $n = 5$, $^*P < 0.05$. one-way ANOVA with Tukey's multiple comparisons test. Error bars in (A) and (B) indicate SEM. (**C**) Kaplan-Meier survival curve of *Il1r1* HET and KO, *Col1a1*$^{\Delta il1r1}$, *Col1a1*$^{WT/loxP}$, *Grem1*$^{\Delta il1r1}$, *Grem1*$^{WT/loxP}$, *Pdgfra*$^{\Delta Il1r1}$, and *Pdgfra*$^{WT/loxP}$ mice after infection with *C. rodentium*. Solid lines represent the WT/loxP controls. $n = 8$, $^*P < 0.05$, $^{***}P < 0.005$, and $^{****}P < 0.001$, log-rank Mantel-Cox test.

Crypt length, the number of proliferating cells per crypt, and the expression of *Ly6a*, a marker of transit amplifying progenitors, were all decreased in *Il1r1* KO and *Col1a1*$^{\Delta il1r1}$ mice (fig. S11, A to D), indicative of reduced expansion of transit amplifying cells. Furthermore, at day 3 after infection when there was increased *Il22* expression in *Il1r1* HET mice, *Krt20*, a marker of terminally differentiated enterocytes, was reduced, reinforcing that IL-22–mediated hyperplasia was dependent on IL-1R1–mediated signaling. These data demonstrate that IL-1R1–dependent induction of RSPO3 in GREM$^+$ mesenchymal cells and IL-22 in ILCs are both required for an optimal host response to *C. rodentium*–induced infection.

IL-1R1–dependent signaling and RSPO3 contribute to epithelial repair after DSS-induced damage

To explore the contribution of IL-1R1–dependent signaling in response to chemically induced cellular damage, we used the dextran sulfate sodium (DSS)–induced colitis model. Loss of IL-1R1 (Fig. 6A) and RSPO3 inactivation (Fig. 6B) both increase susceptibility, but unlike *C. rodentium* infection, neutralization of IL-22 did not induce susceptibility in this model (Fig. 6C). Consistent with these results, DSS-induced up-regulation of *Reg3g* started 10 days after DSS administration, whereas *Reg3g* induced by *C. rodentium* infection peaked at day 3 (Fig. 6D). DSS treatment resulted in an increased early loss of *Lgr5* and *Axin2* and an increased expression of *Rspo3* when compared with *C. rodentium* infection (Fig. 6E). *Il1r1* KO mice exhibited a strongly reduced regenerative response in DSS as compared with *Il1r1* HET mice as shown by a reduction in *Lgr5*, *Rspo3*, and *Axin2* (Fig. 6F). This appeared to be specific to Wnt target genes as *Hopx* expression was unchanged between genotypes (fig. S12) (*36*). Consistent with a reduced regenerative response, crypt density was significantly reduced in *Il1r1* KO compared with *Il1r1* HET mice and more pronounced after DSS treatment compared with *C. rodentium* infection (Fig. 6G). Using *Col1a1*$^{\Delta il1r1}$, *Col1a1*$^{WT/loxP}$, *Grem1*$^{\Delta il1r1}$, and *Grem1*$^{WT/loxP}$ mice, we explored the contribution of IL-1R1–dependent signaling in the COL1A1- and GREM1-positive mesenchymal cell populations in mounting a response to DSS administration. Unlike in the *C. rodentium* model, *Col1a1*$^{\Delta il1r1}$ and *Grem1*$^{\Delta il1r1}$ mice were both sensitive to DSS, recapitulating the germline *Il1r1* KO phenotype in survival, crypt density, and *Lgr5* and *Rspo3* expression (Fig. 7, A to C). Thus, in contrast to the IL-22–dependent *C. rodentium* model, IL-1R1–dependent signaling in RSPO3-producing *Grem1*$^+$ cells alone is required for recovery from DSS-induced damage.

DISCUSSION

Multiple stromal subtypes have been identified in the intestine as important sources of trophic factors required for intestinal homeostasis and regeneration (*6*–*10*, *12*–*16*). Although it is well accepted that stromal cells are critical for supporting epithelial repair, it remains unclear what triggers the response of these niche cells to adaptively regulate progenitor cell proliferation while protecting the stem cell compartment. Even less clear is how different repair mechanisms are enlisted after distinct types of damage. Our data reveal that IL-1R1 plays a key role in orchestrating both processes in a damage-specific manner (Fig. 8). In the setting of *C. rodentium* infection, IL-1R1 activation in GREM1$^+$ mesenchymal cells leads to the up-regulation of RSPO3 production to drive ISC maintenance, whereas IL-1R1 activation in ILCs contributes to epithelial repair through the promotion of IL-22–driven progenitor cell proliferation. In a model of DSS-induced colitis, IL-1 stimulation of GREM1$^+$ *Rspo3*-expressing cells is sufficient to support epithelial repair. Thus, IL-1R1 activation in distinct cell types results in a versatile epithelial response calibrated to the type of damage. This difference in IL-1R1–dependent response may reflect the different nature of the insult. *C. rodentium* uses a type III secretion system that kills a wide range of host epithelial cells and requires rapid mobilization of both IL-22 and RSPO3 to provide an acute life-saving response. DSS acts as a direct toxin to colonic epithelial cells and reduces self-renewal of colonic crypt stem cells (*26*), but its action is more gradual and does not elicit an acute response. How *C. rodentium* virulence factors and DSS toxin trigger IL-1 release could potentially contribute to a

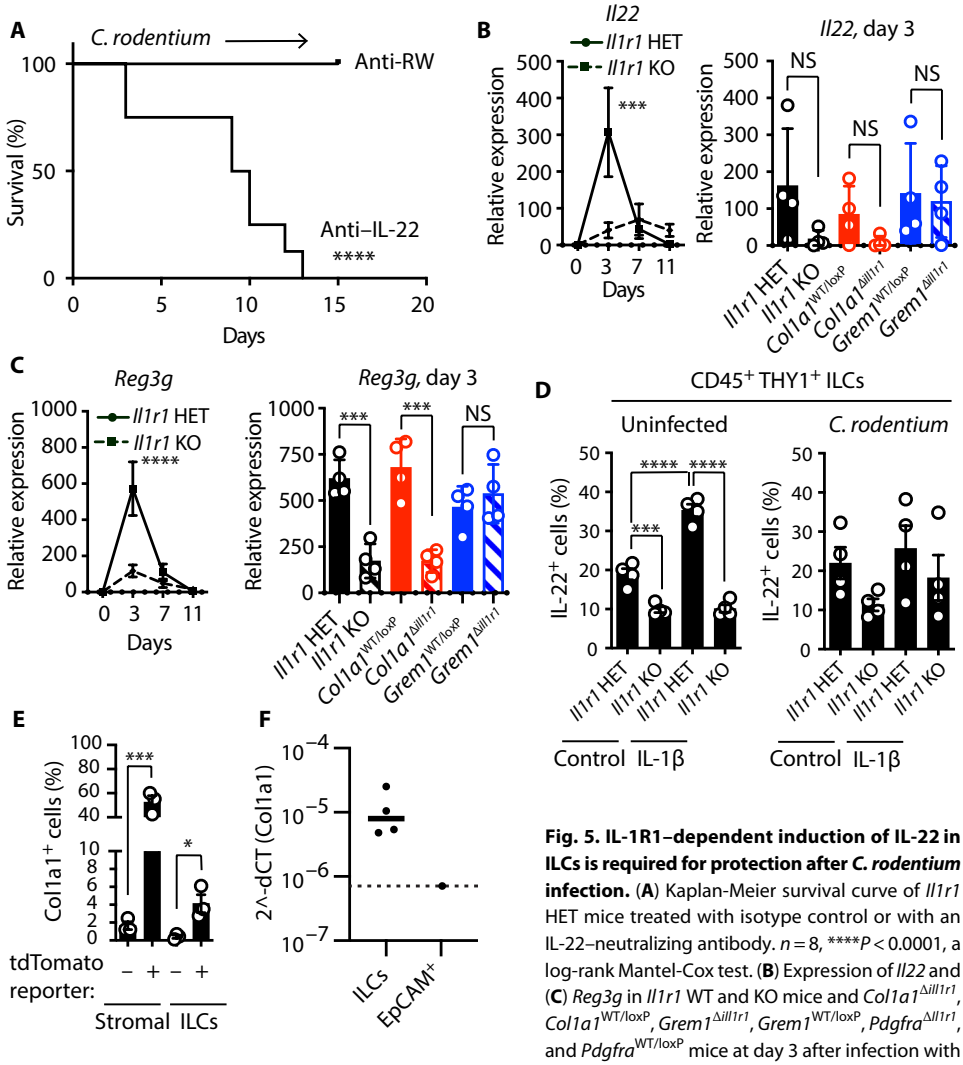

Fig. 5. IL-1R1–dependent induction of IL-22 in ILCs is required for protection after *C. rodentium* infection. (**A**) Kaplan-Meier survival curve of *Il1r1* HET mice treated with isotype control or with an IL-22–neutralizing antibody. $n = 8$, $^{****}P < 0.0001$, a log-rank Mantel-Cox test. (**B**) Expression of *Il22* and (**C**) *Reg3g* in *Il1r1* WT and KO mice and *Col1a1*$^{\Delta il1r1}$, *Col1a1*$^{WT/loxP}$, *Grem1*$^{\Delta il1r1}$, *Grem1*$^{WT/loxP}$, *Pdgfra*$^{\Delta il1r1}$, and *Pdgfra*$^{WT/loxP}$ mice at day 3 after infection with *C. rodentium*. $n = 4$. $^{*}P < 0.05$, $^{**}P < 0.01$, $^{***}P < 0.001$, and $^{****}P < 0.0001$ one-way ANOVA with Tukey's multiple comparisons test. (**D**) Percentage of IL-22$^+$ ILCs of a total pool of THY2$^+$ ILCs isolated from naïve mice 3 days after *C. rodentium* infection of *Il1r1* HET and KO mice and subsequently stimulated with vehicle or IL-1β for 3 hours. $n = 4$. $^{***}P < 0.005$ and $^{****}P < 0.001$, one-way ANOVA with Tukey's multiple comparisons test. (**E**) Percentage of *Col1a1*-expressing stromal cells and ILCs isolated from *Col1a1*.creERT2 (–) or *Col1a1*.creERT2 *Rosa26.lsl.tdTomato* (+) reporter mice after both strains received 4-OHT. $n = 3$. $^{*}P < 0.05$ and $^{***}P < 0.005$, one-way ANOVA with Tukey's multiple comparisons test. (**F**) qPCR of *Col1a1* in sorted Thy-1$^+$ IL-22$^+$ tdTomato$^+$ ILCs and EpCAM$^+$ colon epithelial cells. Error bars in (B) to (E) indicate SEM. Dots in every experiment represent data obtained from independent mice. Experiments were repeated at least twice with similar results. In (B), (C), (E), and (F), 4-OHT was administered for three consecutive days before oral gavage with *C. rodentium*. After infection, mice were treated every third day with 4-OHT.

better understanding of how the nature of the injury triggers different responses downstream of IL-1R1 signaling.

Recent studies have highlighted the emerging heterogeneity and functional roles of intestinal mesenchymal populations. These include FOXL1$^+$ cells, termed telocytes (*14*), and GLI1-expressing mesenchymal cells (*9*). Both have been proposed as sources of Wnt ligands and may be partly overlapping (*10*, *37*). IL-1R1 signaling is not required in Wnt-producing *Pdgfra*$^+$ cells, consistent with the absent up-regulation in general Wnt target genes, and does not appear to drive epithelial repair through increased numbers of committed intestinal progenitor cells, such as *Hopx*$^+$, that can dedifferentiate to replenish the pool of lost stem cells (*36*). IL-1R1 signaling is critical in GREM1$^+$ cells where it drives an increase in RSPO3 production that leads to an up-regulation of the Wnt ISC gene signature. This highlights the adaptability of the processes used to promote intestinal repair where distinct signaling pathways acting on distinct immune and mesenchymal populations are required to generate the appropriate response to the diverse environmental insults present in the intestine.

Colonic epithelial repair in response to damage remains a poorly understood process despite the importance of successful mucosal healing in achieving long-term remission for patients with IBD (*16*, *38*). Recent evidence suggests that increased crypt damage and impaired stem cell self-renewal constitute an important component of IBD pathophysiology (*39*). Improved understanding of the signaling pathways acting on distinct immune and mesenchymal populations to promote epithelial repair may expand current therapeutic opportunities. There is growing evidence pointing to a function of IL-1 in epithelial regeneration. In addition to a role in the skin (*19*) and lung (*17*), we now demonstrate that IL-1 is a key node orchestrating a reparative response in the intestine. Defining the cellular and mechanistic basis for an IL-1–dependent regenerative response in the injured intestinal epithelium may support therapeutic approaches to improve epithelial barrier function in disease.

MATERIALS AND METHODS

Study design

The study was designed to identify radioresistant cells responsible for IL-1R1–dependent support of epithelial restitution after infection- and chemically induced damage. The impact of deleting *Il1r1*, the common receptor for the cytokines IL-1α and IL-1β, in specific subpopulations of cells was based on (i) measurements of epithelial and stem cell markers in whole tissues obtained at predefined endpoints and (ii) survival of the mice, which was defined as mice that were moribund or lost 20% or more of their body weight. Neutralizing antibodies IL-1α, IL-1β, IL-22, and RSPO3 were delivered intraperitoneally. For all studies, mice were randomized on the basis of weights over the treatment groups. The sample size is based on a power analysis that takes into account the predicted size of the effect and the number of experimental groups in any given study. Experiments that measured body weights as an endpoint were carried out in a blinded manner. Bodyweights were monitored for at least 14 days after infection or

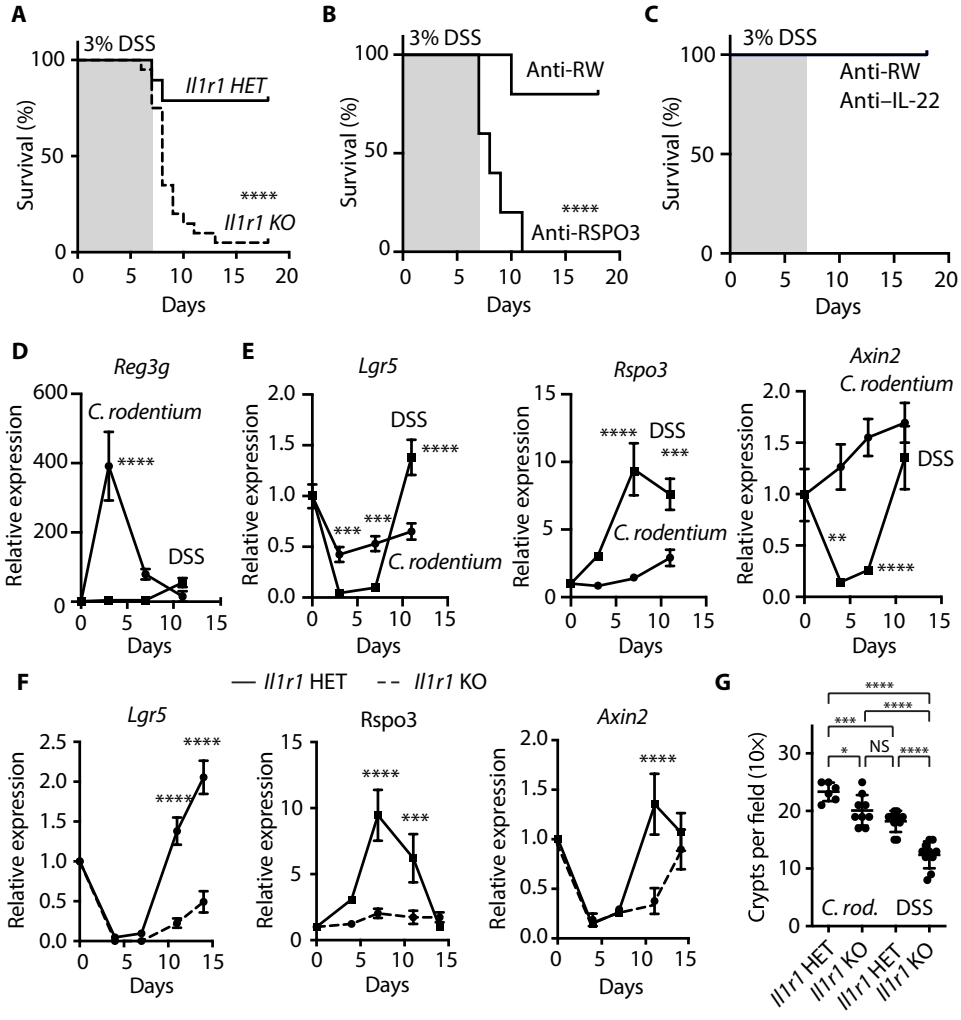

Fig. 6. IL-1R1–dependent signaling and RSPO3 contribute to epithelial repair after DSS-induced damage. (**A**) Kaplan-Meier survival curve of *Il1r1* HET and KO mice after DSS administration. $n = 10$, $^{****}P < 0.0001$, log-rank Mantel-Cox test. (**B**) Kaplan-Meier survival curve of WT mice treated with anti-ragweed (anti-RW) or anti-RSPO3 antibodies. $n = 10$, $^{****}P < 0.0001$, log-rank Mantel-Cox test. (**C**) Kaplan-Meier survival curve of WT mice treated with anti-RW or anti–IL-22 antibodies. $n = 10$, NS log-rank Mantel-Cox test. (**D**) qRT-PCR of *Reg3g* expression in bulk colonic tissue isolated from mice treated with DSS or infected with *C. rodentium*. $n = 4$, $^{****}P < 0.001$, multiple *t* tests. (**E**) qRT-PCR of *Rspo3*, *Lgr5*, and *Axin2* expression in bulk colonic tissue isolated from mice treated with DSS or infected with *C. rodentium*. $n = 4$, $^{***}P < 0.005$, and $^{****}P < 0.001$, one-way ANOVA with Tukey's multiple comparisons test. (**F**) qRT-PCR of *Lgr5*, *Rspo3*, and *Axin2* expression in bulk colonic tissue isolated from *Il1r1* WT and KO mice. $N = 4$, $^{***}P < 0.005$, $^{****}P < 0.001$. (**G**) Comparison of crypt density in *Il1r1* HET or KO mice after *C. rodentium* infection and DSS administration. $N = 6$ (*Il1r1* HET *C. rodentium*), 9 (*Il1r1* KO *C. rodentium*), 10 (*Il1r1* HET and KO DSS). $^{*}P < 0.05$, $^{***}P < 0.001$, and $^{****}P < 0.0001$. Error bars in (D) to (G) indicate SEM.

DSS administration, and mice that lost 20% or more of their body weights were euthanized following the Institutional Animal Care and Use Committee (IACUC) standards. Assessment of endpoints including quantitative polymerase chain reaction (qPCR), in vitro coculture, and ISH was not performed in a blinded fashion. All experiments were repeated at least twice, and results from all experiments, with outliers included, are displayed in the data file (table S4).

Mice

A conditional allele of *Il1r1* was created by introducing *loxP* sites flanking exons 3 and 4 by two consecutive rounds of cytoplasmic co-injection of *Cas9* mRNA, single guide RNA (sgRNA), and single-stranded DNA (ssDNA) oligo donors containing *loxP* sites into C57BL/6N zygotes. The resulting mosaic founders were screened for absence of editing at the top algorithm-predicted off-targets, as previously described (*40*). After each round of microinjection, mosaic founders without off-targets were bred to C57BL/6N for germline transmission. Heterozygous progenies carrying the final conditional KO (loxP) allele were then crossed to mice carrying cre. The sgRNA sequences used to target *Il1r1* introns 2 and 4, respectively, are 5′-ACAACTGGAGAGTGTACACA and 5′-GAATATTGCTCTCTTTGTAG. The 746–base pair floxed region corresponds to GRCm38/mm10 chr1:40,292,998-40,293,743. Genotyping was carried out using the following primers: AGGAACTGACTGTAAATGAT, TTAGCATCATTGGTTAGTAAAG, and ACTAAGGCAGATAGAGACA. *Col1a1*.creERT2.*ALPP* mice were obtained from the Jackson Laboratory [B6.Cg-Tg(Col1a1-cre/ERT2)1Crm/J, stock 016241] (*41*) and crossed to *Rosa26.lsl.tdTomato* mice (Jackson Laboratory, stock 007914), (*42*) to generate *Col1a1*.creERT2 *Rosa26.lsl.tdTomato* reporter mice and backcrossed for 10 generations to C57BL/6N mice. Mice were then crossed to *Il1r1* loxP/loxP mice to create an inducible *Il1r1* KO in *Col1a1*-expressing stromal cells (*Col1a1*.creERT2 *Il1r1* loxP/loxP or *Col1a1*$^{\Delta iIl1r1}$). *Pdgfra*.cre mice were obtained from the Jackson Laboratory (stock no. 013148) and crossed to *Il1r1* loxP/loxP mice to create *Pdgfra*.cre *Il1r1* loxP/loxP (*Pdgfra*$^{\Delta iIl1r1}$) and WT/loxP mice (*Pdgfra*$^{WT/loxP}$). *Grem1*.creERT2 mice were generated as described previously (*29*) and crossed to *Rosa26*-EYFP (006148; Jackson Laboratory) to generate *Grem1*.Cre-ERT2 *Rosa26*-LSL-EYFP mice. *Grem1*.creERT2 mice were crossed to *Il1r1* loxP/loxP mice to generate *Grem1*.creERT2 *Il1r1* loxP/loxP (*Grem1*$^{\Delta iIl1r1}$) and WT/loxP (*Grem1*$^{WT/loxP}$) mice. Successful deletion of *Il1r1* by Cre-induced recombination was confirmed by quantitative reverse transcription PCR (qRT-PCR) after sorting out primary colonic fibroblasts isolated from *Grem1*$^{WT/loxP}$ and *Grem1*$^{\Delta iIl1r1}$ mice treated with 4-hydroxytamoxifen (4-OHT). In all experiments, only littermates that were hemizygous or heterozygous for Cre were used. All protocols described herein were approved by the Genentech IACUC. *Il1r1*$^{-/-}$ mice (B6.129S7-*Il1r1*$^{tm1Imx/J}$) (*43*) were obtained from Jackson Laboratory (stock 003245) and backcrossed for eight generations to C57BL6/J mice (Jackson Laboratory).

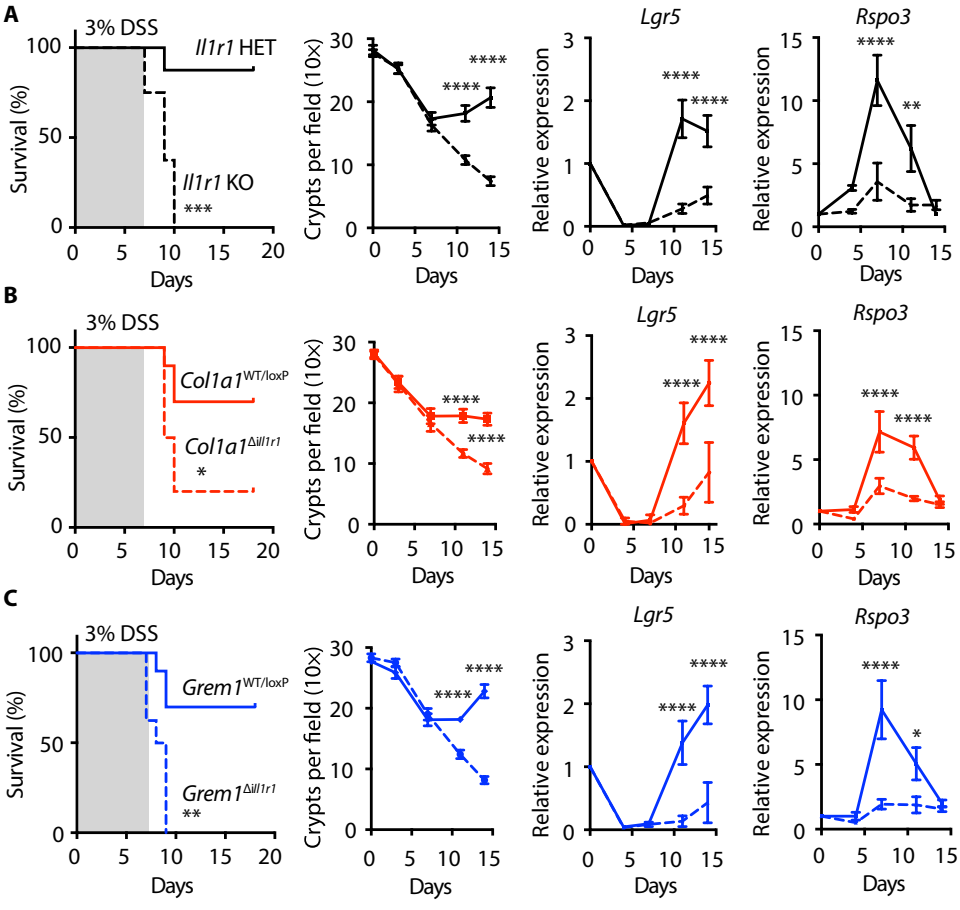

Fig. 7. IL-1R1–dependent induction of RSPO3 in *Grem1*$^{+}$ cells is required for stem cell renewal and survival after DSS-induced epithelial damage. (**A** to **C**) Kaplan-Meier survival curve, crypt density, and qRT-PCR gene expression of *Lgr5* and *Rspo3* in *Il1r1* WT and KO mice (A) and *Col1a1*$^{\Delta il1r1}$ (B) and *Grem1*$^{\Delta il1r1}$ mice (C) after DSS treatment. Solid lines represent heterozygous (*Il1r1* strain), *Col1a1*$^{WT/loxP}$, or *Grem1*$^{WT/loxP}$ mice; dotted lines represent KO (*Il1r1* strain), *Col1a1*$^{\Delta il1r1}$, or *Grem1*$^{\Delta il1r1}$ mice. $N = 10$, $^{*}P < 0.05$, $^{**}P < 0.01$, and $^{***}P < 0.005$, log-rank Mantel-Cox test. $N = 4$, $^{****}P < 0.0001$, one-way ANOVA with Tukey's multiple comparisons test. Error bars indicate SEM. 4-OHT was administered for three consecutive days before and every third day after DSS administration. Experiments were repeated at least twice with similar results.

Tamoxifen administration for in vivo studies:

To delete *Il1r1* in *Col1a1*.creERT2 or *Grem1*.creERT2 strains, mice were treated with 4-OHT (60 mg/kg) for three consecutive days before oral gavage with *C. rodentium* or DSS administration. After infection with *C. rodentium* or DSS administration, mice were treated every third day with 4-OHT. For all experiments, bodyweights were monitored for at least 14 days after infection or DSS administration, and mice that lost 20% or more of their body weights were euthanized following IACUC standards.

DSS-induced colitis

Three percent (w/w) colitis-grade DSS (MP Biomedicals, 9011-18-1) was added to the drinking water for 7 days. The water was weighed daily to determine the average water consumption per cage. Mouse bodyweights were recorded daily, and mice that lost 20% or more of their body weights were euthanized following IACUC standards. In the anti-RSPO3 and anti–IL-22 treatment groups, mice were injected intraperitoneally every third day with a specific antibody (15 mg/kg) against RSPO3 (*28*), anti–IL-22 (*30*), or anti-ragweed as a vehicle control (Genentech) starting on the first day of DSS administration.

Quantification of crypt density

Images of hematoxylin and eosin (H&E)–stained 6-μm paraffin sections of the colon were collected at ×10 magnification and used to quantify the number of crypts in 1500-μm randomly selected longitudinal segments of the distal colon.

Infection with *C. rodentium* and treatment

C. rodentium was purified on MacConkey agar, and one colony was inoculated in LB and allowed to grow overnight to produce a stock solution. Mice were then inoculated by oral gavage with 2×10^{9} colony-forming units of *C. rodentium*. For the anti–IL-1 experiments, mice were injected intraperitoneally every third day with a specific antibody (15 mg/kg) against IL-1α (Bio X Cell, ALF-161) or IL-1β (Genentech Inc.). For the anti-RSPO3 experiments, mice were injected intraperitoneally every third day with a specific antibody (15 mg/kg) against RSPO3 (*28*) or anti-ragweed as a vehicle control (Genentech Inc.). For the recombinant RSPO3 rescue experiments, mice were injected intraperitoneally every third day with 0.1 ml of recombinant RSPO3 (Genentech Inc.; 300 μg per mouse per dose) or the equivalent volume of phosphate-buffered saline (PBS) used as a vehicle control. For the anti–IL-22 experiments, mice were injected intraperitoneally every third day with a specific antibody (15 mg/kg) against IL-22 (*30*).

Quantitative reverse transcription polymerase chain reaction

Colons were isolated, flushed with PBS, and small pieces dissected from the distal colon were placed in RNAlater. The tissue pieces were then homogenized using a TissueLyser 2, and RNA was isolated with an RNeasy Mini Kit (Qiagen, 74104). DNA was degraded on a column with ribonuclease-free deoxyribonuclease (Qiagen, 79254), and complementary DNA (cDNA) was synthesized with the iScript cDNA synthesis kit (Bio-Rad, 1708891). For cDNA synthesis, between 200 and 500 ng of starting RNA was used for each reaction. For qRT-PCR, TaqMan Fast Advanced Master Mix (Qiagen) was used.

Isolation of primary intestinal fibroblasts

The colon was removed, flushed, splayed open lengthwise, and cut into ~1 cm by 1 cm pieces before processing according to the lamina propria kit from Miltenyi Biotec. Briefly, the colon pieces were placed in a 50-ml conical tube with 20 ml of predigestion solution

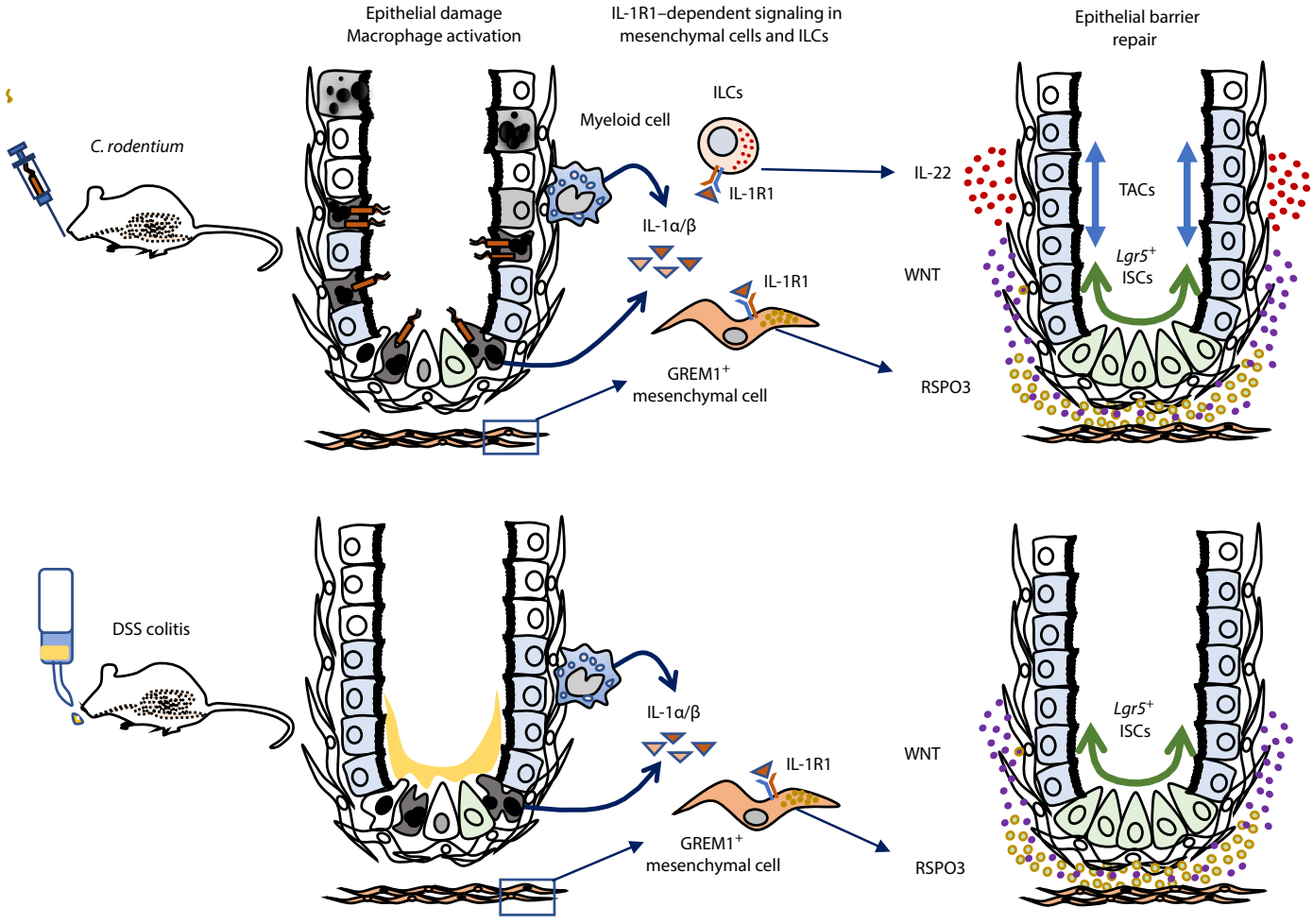

Fig. 8. IL-1R1–dependent signaling coordinates epithelial regeneration. Diagram demonstrating how IL-1R1–dependent signaling orchestrates distinct repair programs required to restore intestinal epithelial barrier function after *C. rodentium* or DSS-induced intestinal injury. TACs, transit amplifying cells.

[1× Hanks' balanced salt solution (HBSS) with 5 mM EDTA, 5% fetal bovine serum (FBS), and 1 mM dithiothreitol (DTT)] and incubated three times at 37°C in a MACSmix tube rotator for 20 min each (changing the solution each time). Afterward, the colon pieces were vortexed for 10 s and passed through a 100-μm strainer to remove any cellular debris. The colon pieces were placed into a gentleMACS C tube along with the enzyme mix and dissociated according to the LPDK protocol from Miltenyi. After dissociation, the tissue solution was washed twice in 25 ml of high-glucose Dulbecco's modified Eagle's medium (DMEM) and spun down at 300 rcf to pellet the cells. The cells were then resuspended into a 100-mm tissue culture dish and incubated at 37°C in high-glucose DMEM with 10% FBS, 10 mM Hepes, penicillin and streptomycin, and 1× GlutaMax. The media was changed after 1 day to remove cellular debris, and the cells were used within 3 days after isolation for downstream analysis.

Isolation of primary epithelial organoids

Primary epithelial organoids were collected as follows: Colon tissue was isolated, flushed with PBS, filleted, and cut into ~1 cm by 1 cm pieces. After dissection, the tissue pieces were washed in PBS three times or until the PBS was clear to remove the mucus layer. Afterward, the tissue pieces were incubated for 5 min at 37°C in PBS with 2.5 mM EDTA to dissociate epithelial cells. After incubation, the tissue pieces were mixed gently and then strained from the solution. The tissue pieces were then resuspended in PBS with 5 mM EDTA and incubated for 5 min at 37°C. After incubation, the tissue pieces were shaken to dislodge epithelial crypts, the supernatant was filtered through a 100-μm filter, and the solution was spun down to pellet the cells. After centrifugation, the cell pellet was washed with 25 ml of DMEM without serum to remove excess EDTA and centrifuged once more to pellet the cells. After the final centrifugation, the cells were resuspended in a 50:50 solution of media and Matrigel, and 50 μl was plated into each well of a 24-well plate. The Matrigel solution was allowed to solidify at 37°C for 30 min before adding 500 μl of stem cell media (STEMCELL Technologies, catalog no. 06005).

Epithelial organoid and primary fibroblast coculture

For the fibroblast and epithelial organoid coculture, separate cultures of epithelial organoids and primary fibroblasts were dissociated, spun down at 300 rcf, and resuspended in stem cell media. Both organoids and fibroblasts were then mixed at a ratio of 1:1, placed in 50% Matrigel, and cultured at 37°C. The coculture was incubated for 4 days in full stem cell media to allow the organoids to mature

and bud before changing to minimal media (DMEM alone, DMEM + IL-1α or IL-1β, or DMEM + IL-1α or IL-1β + anti-RSPO3). IL-1α and IL-1β (R&D) were used at 10 ng/ml, and anti-RSPO3 was used at 10 μg/ml.

In situ hybridization

ISH was performed using reagents and protocols from Advanced Cell Diagnostics. Briefly, the colon was longitudinally cut through the midline and fixed in 10% neutral buffered formalin for 24 hours before being placed in 70% ethanol and processed for paraffin embedding. Sections at 6 μm thickness were cut through the midline and perpendicular to the colon lumen and then allowed to dry in a 60°C oven for 1 hour. Sections were rehydrated in two washes of xylene for 5 min each followed by two washes in 100% ethanol, one wash in 95% ethanol, and one wash in 90% ethanol, all for 1 min each. After rehydration, the samples were incubated in hydrogen peroxide, boiled in antigen retrieval buffer, and then digested with proteinase for 15 min at 40°C. After digestion, the slides were washed twice for 1 min with ISH wash buffer and then hybridized with probes for 2 hours at 40°C. After hybridization, amplification steps were completed according to Advanced Cell Diagnostics protocol. After the final amplification incubation, the slides were washed in ISH wash buffer and detected with horseradish peroxidase conjugated with DAB, counterstained with hematoxylin, and then baked in a 60°C oven for 15 min before mounting with nonaqueous mounting media.

Fluorescence-activated cell sorting

The colon was removed, any remaining fat was trimmed off, and the tissue was dissociated following the Miltenyi lamina propria kit. Briefly, the colon was cut lengthwise to open it and then cut into small squares about 0.5 cm by 0.5 cm in size. The tissue was then placed in a 50-ml conical tube with 20 ml of predigestion solution (HBSS with 5 mM EDTA, 5% FBS, and 1 mM DTT) and incubated for 20 min at 37°C while rotating. The tissue was then strained, and the process was repeated twice more, once again with predigestion solution and once with HBSS, straining after each step. The enzyme solution was then reconstituted according to the protocol, and the tissue and enzyme solution were collected in a gentleMACS tube and dissociated according to the LPDK protocol from Miltenyi. After dissociation, the tube was centrifuged at 300*g* for 5 min, and the supernatant was poured off. The dissociated cells were then washed twice with fluorescence-activated cell sorting (FACS) buffer, strained through a 100 μM and 40 μM filter. Dissociated single cells were then subsequently stained for flow cytometry analysis.

For IL-1β stimulation of ILCs, ~250,000 cells were resuspended into a 96-well plate and resuspended in DMEM with 1 ng of IL-1β or control vehicle. The cells were then stimulated for 3 hours before washing and preparing for antibody staining.

For surface marker antibody staining, ~250,000 cells were resuspended into a 96-well 1-ml plate and incubated with FACS buffer with Fc block (1:10) and live/dead stain (1:1000) for 10 min. After blocking, the primary antibodies were added to each well at a 1:100 dilution and stained for at least 30 min. The cells were then washed twice with FACS buffer, spinning at 300*g* for 5 min after each wash.

For intracellular staining of IL-22, cells were fixed with BD Cytofix (catalog no. 554722). After fixation, cells were washed twice with BD Perm/Wash buffer and then stained with anti–IL-22 antibody (1:100 dilution) in a BD Perm/Wash buffer dilution 1:10. Cells were stained for 1 hour before washing twice with BD Perm/Wash buffer, resuspended in FACS buffer, and processed.

Single-cell RNA sequencing data analysis

Gene expression matrices containing single-cell RNA sequencing data from colonic tissue from five healthy controls and five patients diagnosed with ulcerative colitis (*15*) were imported into Partek Flow Genomic Analysis Software (Copyright 2016, Partek Inc., St. Louis, MO). A subsample of cells expressing either *GREM1* or *PDGFRA*, at least 0.5 and 0.75 reads per kilobase of transcript, per million mapped reads (RPKM), respectively, was selected and reclustered using the Seurat software package (*44*, *45*). Cell subsets were defined and labeled by t-distributed stochastic neighbor embedding clustering. Data visualization for the subsample of cells expressing *GREM1* or *PDGFRA* was imported into R and generated with the ggplot2 package (*46*).

Statistical analysis

All data were analyzed and graphed using Prism 6 software (GraphPad). All survival curves were analyzed with a log-rank Mantel-Cox test and had at least $n = 5$ animals per experimental group. Comparisons between two groups were analyzed by performing an unpaired two-tailed Student's *t* test. Comparisons between more than two groups were analyzed by performing a one-way analysis of variance (ANOVA) with Tukey's multiple comparisons test. For all experiments, individual dots on each graph represents unique biological samples and not technological replicates. For marking significance, $^{*}P < 0.05$, $^{**}P < 0.01$, $^{***}P < 0.005$, and $^{****}P < 0.001$ or 0.0001 as indicated in the legends. All experiments were performed at least twice. Error bars indicate SEM.

SUPPLEMENTARY MATERIALS

immunology.sciencemag.org/cgi/content/full/6/59/eabe8856/DC1

Fig. S1. Susceptibility of *Il1r1* WT and HET mice to *C. rodentium* and differential regulation of cytokines in *Il1r1* HET and KO mice after *C. rodentium* infection.

Fig. S2. Contribution of IL-1α and IL-1β to host resistance against *C. rodentium* infection and activation of colon mesenchymal cells by IL-1α and IL-1β.

Fig. S3. Effect of recombinant RSPO3 on *Lgr5* expression and crypt density in *C. rodentium*–infected $Il1r1^{-/-}$ KO mice.

Fig. S4. ISH of *Rspo3* in uninfected and *C. rodentium* infected mice.

Fig. S5. *Grem1* and *Pdgfra* coexpression and gating strategy for isolating $GREM1^{+}$ and $PDGFR\alpha^{+}$ mesenchymal cells.

Fig. S6. Workflow of scRNA-seq analysis of $GREM1^{+}$ and $PDGFRA^{+}$ cell populations in human colonic biopsies from healthy control and ulcerative colitis diagnosed donors.

Fig. S7. Overview of different *Cre* lines used in our studies.

Fig. S8. Characterization of *Il1r1* KO, $Col1a^{WT/WT}$, $Col1a1^{\Delta Il1r1}$, $Pdgfra^{WT/WT}$, $Pdgfra^{\Delta Il1r1}$, $Grem1^{WT/WT}$, and $Grem1^{\Delta Il1r1}$ mice.

Fig. S9. IL-1R1–dependent increase in $GREM1^{+}$ cells.

Fig. S10. Gating strategy for evaluating *Col1a1* expression in ILCs and mesenchymal cells.

Fig. S11. Colon hyperplasia in *Il1r1* WT and KO mice.

Fig. S12. Expression of *Hopx* in the colon of naïve mice and after DSS treatment.

Table S1. Sequences of qPCR primers and probes.

Table S2. Catalog numbers of ISH probes.

Table S3. Catalog numbers of antibodies.

Table S4. Raw data file (Excel spreadsheet).

View/request a protocol for this paper from *Bio-protocol*.

REFERENCES AND NOTES

1. J. A. Knoblich, Mechanisms of asymmetric stem cell division. *Cell* **132**, 583–597 (2008).
2. H. F. Farin, I. Jordens, M. H. Mosa, O. Basak, J. Korving, D. V. Tauriello, K. de Punder, S. Angers, P. J. Peters, M. M. Maurice, H. Clevers, Visualization of a short-range Wnt gradient in the intestinal stem-cell niche. *Nature* **530**, 340–343 (2016).
3. J. Zhao, X. Chen, G. Song, J. Zhang, H. Liu, X. Liu, Uhrf1 controls the self-renewal versus differentiation of hematopoietic stem cells by epigenetically regulating the cell-division modes. *Proc. Natl. Acad. Sci. U.S.A.* **114**, E142–E151 (2017).

4. J. Wang, Q. Sun, Y. Morita, H. Jiang, A. Gross, A. Lechel, K. Hildner, L. M. Guachalla, A. Gompf, D. Hartmann, A. Schambach, T. Wustefeld, D. Dauch, H. Schrezenmeier, W. K. Hofmann, H. Nakauchi, Z. Ju, H. A. Kestler, L. Zender, K. L. Rudolph, A differentiation checkpoint limits hematopoietic stem cell self-renewal in response to DNA damage. *Cell* **158**, 1444 (2014).
5. C. Q. Doe, Neural stem cells: Balancing self-renewal with differentiation. *Development* **135**, 1575–1587 (2008).
6. Z. Kabiri, G. Greicius, B. Madan, S. Biechele, Z. Zhong, H. Zaribafzadeh, Edison, J. Aliyev, Y. Wu, R. Bunte, B. O. Williams, J. Rossant, D. M. Virshup, Stroma provides an intestinal stem cell niche in the absence of epithelial Wnts. *Development* **141**, 2206–2215 (2014).
7. I. Stzepourginski, G. Nigro, J. M. Jacob, S. Dulauroy, P. J. Sansonetti, G. Eberl, L. Peduto, $CD34^+$ mesenchymal cells are a major component of the intestinal stem cells niche at homeostasis and after injury. *Proc. Natl. Acad. Sci. U.S.A.* **114**, E506–E513 (2017).
8. T. Valenta, B. Degirmenci, A. E. Moor, P. Herr, D. Zimmerli, M. B. Moor, G. Hausmann, C. Cantu, M. Aguet, K. Basler, Wnt ligands secreted by subepithelial mesenchymal cells are essential for the survival of intestinal stem cells and gut homeostasis. *Cell Rep.* **15**, 911–918 (2016).
9. B. Degirmenci, T. Valenta, S. Dimitrieva, G. Hausmann, K. Basler, GLI1-expressing mesenchymal cells form the essential Wnt-secreting niche for colon stem cells. *Nature* **558**, 449–453 (2018).
10. G. Greicius, Z. Kabiri, K. Sigmundsson, C. Liang, R. Bunte, M. K. Singh, D. M. Virshup, PDGFRα pericryptal stromal cells are the critical source of Wnts and RSPO3 for murine intestinal stem cells in vivo. *Proc. Natl. Acad. Sci.* **115**, E3173–E3181 (2018).
11. J. Beumer, H. Clevers, Regulation and plasticity of intestinal stem cells during homeostasis and regeneration. *Development* **143**, 3639–3649 (2016).
12. M. Roulis, C. Nikolaou, E. Kotsaki, E. Kaffe, N. Karagianni, V. Koliaraki, K. Salpea, J. Ragoussis, V. Aidinis, E. Martini, C. Becker, H. R. Herschman, S. Vetrano, S. Danese, G. Kollias, Intestinal myofibroblast-specific Tpl2-Cox-2-PGE2 pathway links innate sensing to epithelial homeostasis. *Proc. Natl. Acad. Sci. U.S.A.* **111**, E4658–E4667 (2014).
13. R. Aoki, M. Shoshkes-Carmel, N. Gao, S. Shin, C. L. May, M. L. Golson, A. M. Zahm, M. Ray, C. L. Wiser, C. V. Wright, K. H. Kaestner, Foxl1-expressing mesenchymal cells constitute the intestinal stem cell niche. *Cell. Mol. Gastroenterol. Hepatol.* **2**, 175–188 (2016).
14. M. Shoshkes-Carmel, Y. J. Wang, K. J. Wangensteen, B. Toth, A. Kondo, E. E. Massasa, S. Itzkovitz, K. H. Kaestner, Subepithelial telocytes are an important source of Wnts that supports intestinal crypts. *Nature* **557**, 242–246 (2018).
15. J. Kinchen, H. H. Chen, K. Parikh, A. Antanaviciute, M. Jagielowicz, D. Fawkner-Corbett, N. Ashley, L. Cubitt, E. Mellado-Gomez, M. Attar, E. Sharma, Q. Wills, R. Bowden, F. C. Richter, D. Ahern, K. D. Puri, J. Henault, F. Gervais, H. Koohy, A. Simmons, Structural remodeling of the human colonic mesenchyme in inflammatory bowel disease. *Cell* **175**, 372–386.e17 (2018).
16. P. Henderson, J. E. van Limbergen, J. Schwarze, D. C. Wilson, Function of the intestinal epithelium and its dysregulation in inflammatory bowel disease. *Inflamm. Bowel Dis.* **17**, 382–395 (2011).
17. H. Katsura, Y. Kobayashi, P. R. Tata, B. L. M. Hogan, IL-1 and TNF-α contribute to the inflammatory niche to enhance alveolar regeneration. *Stem Cell Rep.* **12**, 657–666 (2019).
18. Y. S. Lee, H. Yang, J. Y. Yang, Y. Kim, S. H. Lee, J. H. Kim, Y. J. Jang, B. A. Vallance, M. N. Kweon, Interleukin-1 (IL-1) signaling in intestinal stromal cells controls KC/ CXCL1 secretion, which correlates with recruitment of IL-22- secreting neutrophils at early stages of Citrobacter rodentium infection. *Infect. Immun.* **83**, 3257–3267 (2015).
19. P. Lee, R. Gund, A. Dutta, N. Pincha, I. Rana, S. Ghosh, D. Witherden, E. Kandyba, A. MacLeod, K. Kobielak, W. L. Havran, C. Jamora, Stimulation of hair follicle stem cell proliferation through an IL-1 dependent activation of γδT cells. *eLife* **6**, (2017).
20. A. Song, L. Zhu, G. Gorantla, O. Berdysz, S. A. Amici, M. Guerau-de-Arellano, K. M. Madalena, J. K. Lerch, X. Liu, N. Quan, Salient type 1 interleukin 1 receptor expression in peripheral non-immune cells. *Sci. Rep.* **8**, 723 (2018).
21. S. A. Luperchio, D. B. Schauer, Molecular pathogenesis of Citrobacter rodentium and transmissible murine colonic hyperplasia. *Microbes Infect.* **3**, 333–340 (2001).
22. S. L. Lebeis, K. R. Powell, D. Merlin, M. A. Sherman, D. Kalman, Interleukin-1 receptor signaling protects mice from lethal intestinal damage caused by the attaching and effacing pathogen Citrobacter rodentium. *Infect. Immun.* **77**, 604–614 (2009).
23. Y. Chung, S. H. Chang, G. J. Martinez, X. O. Yang, R. Nurieva, H. S. Kang, L. Ma, S. S. Watowich, A. M. Jetten, Q. Tian, C. Dong, Critical regulation of early Th17 cell differentiation by interleukin-1 signaling. *Immunity* **30**, 576–587 (2009).
24. A. Mantovani, C. A. Dinarello, M. Molgora, C. Garlanda, Interleukin-1 and related cytokines in the regulation of inflammation and immunity. *Immunity* **50**, 778–795 (2019).
25. N. Kayagaki, M. T. Wong, I. B. Stowe, S. R. Ramani, L. C. Gonzalez, S. Akashi-Takamura, K. Miyake, J. Zhang, W. P. Lee, A. Muszynski, L. S. Forsberg, R. W. Carlson, V. M. Dixit, Noncanonical inflammasome activation by intracellular LPS independent of TLR4. *Science* **341**, 1246–1249 (2013).
26. C. Harnack, H. Berger, A. Antanaviciute, R. Vidal, S. Sauer, A. Simmons, T. F. Meyer, M. Sigal, R-spondin 3 promotes stem cell recovery and epithelial regeneration in the colon. *Nat. Commun.* **10**, 4368 (2019).
27. W. de Lau, W. C. Peng, P. Gros, H. Clevers, The R-spondin/Lgr5/Rnf43 module: Regulator of Wnt signal strength. *Genes Dev.* **28**, 305–316 (2014).
28. E. E. Storm, S. Durinck, F. de Sousa e Melo, J. Tremayne, N. Kljavin, C. Tan, X. Ye, C. Chiu, T. Pham, J. A. Hongo, T. Bainbridge, R. Firestein, E. Blackwood, C. Metcalfe, E. W. Stawiski, R. L. Yauch, Y. Wu, F. J. de Sauvage, Targeting PTPRK-RSPO3 colon tumours promotes differentiation and loss of stem-cell function. *Nature* **529**, 97–100 (2016).
29. N. McCarthy, E. Manieri, E. E. Storm, A. Saadatpour, A. M. Luoma, V. N. Kapoor, S. Madha, L. T. Gaynor, C. Cox, S. Keerthivasan, K. Wucherpfennig, G. C. Yuan, F. J. de Sauvage, S. J. Turley, R. A. Shivdasani, Distinct mesenchymal cell populations generate the essential intestinal BMP signaling gradient. *Cell Stem Cell* **26**, 391–402.e5 (2020).
30. Y. Zheng, P. A. Valdez, D. M. Danilenko, Y. Hu, S. M. Sa, Q. Gong, A. R. Abbas, Z. Modrusan, N. Ghilardi, F. J. de Sauvage, W. Ouyang, Interleukin-22 mediates early host defense against attaching and effacing bacterial pathogens. *Nat. Med.* **14**, 282–289 (2008).
31. S. U. Seo, P. Kuffa, S. Kitamoto, H. Nagao-Kitamoto, J. Rousseau, Y. G. Kim, G. Nunez, N. Kamada, Intestinal macrophages arising from CCR2(+) monocytes control pathogen infection by activating innate lymphoid cells. *Nat. Commun.* **6**, 8010 (2015).
32. B. A. Vallance, Mice lacking T and B lymphocytes develop transient colitis and crypt hyperplasia yet suffer impaired bacterial clearance during citrobacter rodentium infection. *Infect. Immun.* **70**, 2070–2081 (2002).
33. C. P. Simmons, S. Clare, M. Ghaem-Maghami, T. K. Uren, J. Rankin, A. Huett, R. Goldin, D. J. Lewis, T. T. MacDonald, R. A. Strugnell, G. Frankel, G. Dougan, Central role for B lymphocytes and $CD4^+$ T cells in immunity to infection by the attaching and effacing pathogen Citrobacter rodentium. *Infect. Immun.* **71**, 5077–5086 (2003).
34. J. K. Bando, M. Colonna, Innate lymphoid cell function in the context of adaptive immunity. *Nat. Immunol.* **17**, 783–789 (2016).
35. Immunological Genome Project, ImmGen at 15. *Nat. Immunol.* **21**, 700–703 (2020).
36. Y. Wang, I. L. Chiang, T. E. Ohara, S. Fujii, J. Cheng, B. D. Muegge, A. Ver Heul, N. D. Han, Q. Lu, S. Xiong, F. Chen, C. W. Lai, H. Janova, R. Wu, C. E. Whitehurst, K. L. VanDussen, T. C. Liu, J. I. Gordon, L. D. Sibley, T. S. Stappenbeck, Long-term culture captures injury-repair cycles of colonic stem cells. *Cell* **179**, 1144–1159.e15 (2019).
37. A. Kondo, K. H. Kaestner, Emerging diverse roles of telocytes. *Development* **146**, dev175018 (2019).
38. E. Martini, S. M. Krug, B. Siegmund, M. F. Neurath, C. Becker, Mend your fences: The epithelial barrier and its relationship with mucosal immunity in inflammatory bowel disease. *Cell. Mol. Gastroenterol. Hepatol.* **4**, 33–46 (2017).
39. I. Dotti, R. Mora-Buch, E. Ferrer-Picón, N. Planell, P. Jung, M. C. Masamunt, R. F. Leal, J. Martín de Carpi, J. Llach, I. Ordás, E. Batlle, J. Panés, A. Salas, Alterations in the epithelial stem cell compartment could contribute to permanent changes in the mucosa of patients with ulcerative colitis. *Gut* **66**, 2069–2079 (2017).
40. K. R. Anderson, M. Haeussler, C. Watanabe, V. Janakiraman, J. Lund, Z. Modrusan, J. Stinson, Q. Bei, A. Buechler, C. Yu, S. R. Thamminana, L. Tam, M. A. Sowick, T. Alcantar, N. O'Neil, J. Li, L. Ta, L. Lima, M. Roose-Girma, X. Rairdan, S. Durinck, S. Warming, CRISPR off-target analysis in genetically engineered rats and mice. *Nat. Methods* **15**, 512–514 (2018).
41. J. E. Kim, K. Nakashima, B. de Crombrugghe, Transgenic mice expressing a ligand-inducible cre recombinase in osteoblasts and odontoblasts: A new tool to examine physiology and disease of postnatal bone and tooth. *Am. J. Pathol.* **165**, 1875–1882 (2004).
42. L. Madisen, T. A. Zwingman, S. M. Sunkin, S. W. Oh, H. A. Zariwala, H. Gu, L. L. Ng, R. D. Palmiter, M. J. Hawrylycz, A. R. Jones, E. S. Lein, H. Zeng, A robust and high-throughput Cre reporting and characterization system for the whole mouse brain. *Nat. Neurosci.* **13**, 133–140 (2010).
43. M. B. Glaccum, K. L. Stocking, K. Charrier, J. L. Smith, C. R. Willis, C. Maliszewski, D. J. Livingston, J. J. Peschon, P. J. Morrissey, Phenotypic and functional characterization of mice that lack the type I receptor for IL-1. *J. Immunol.* **159**, 3364–3371 (1997).
44. A. Butler, P. Hoffman, P. Smibert, E. Papalexi, R. Satija, Integrating single-cell transcriptomic data across different conditions, technologies, and species. *Nat. Biotechnol.* **36**, 411–420 (2018).
45. T. Stuart, A. Butler, P. Hoffman, C. Hafemeister, E. Papalexi, W. M. Mauck III, Y. Hao, M. Stoeckius, P. Smibert, R. Satija, Comprehensive integration of single-cell data. *Cell* **177**, 1888–1902.e21 (2019).
46. H. Wickham, *ggplot2: Elegant Graphics for Data Analysis* (Springer-Verlag, 2016).

Acknowledgments: We thank W. Ouyang for helpful discussions, our colleagues in the Laboratory Animal Resources for help with microinjection and animal breeding, the Genetic Analysis Laboratory for genotyping service, S. Thamminana for help with analysis of the CRISPR-edited allele, and S. Powell and W. Ortiz for maintaining the conditional and global *Il1r1* KO mouse colonies. **Author contributions:** C.B.C. and E.E.S. designed and conducted all

in vivo and in vitro experiments, analyzed the data, and wrote the paper; V.N.K. and S.J.T. characterized the *Grem1*.creERT2 mice and provided expertise in mesenchymal/fibroblast biology; J.C.-S. helped optimize the flow cytometry studies; D.L.L. helped with analyzing scRNA-seq data; L.W. helped generate and optimize the fibroblast-organoid cocultures; Y.L., N.K., and N.O. helped perform the in vivo studies; T.W.B. purified RSPO3; K.A., M.R.-G., and S.W. designed and generated the conditional *Il1r1* KO and *Grem1*.creERT2 mice; J.R.A. supervised the studies and contributed expertise in fibroblast biology; F.J.d.S. and M.v.L.C. conceived and supervised the study, designed the experiments, analyzed the data, and wrote the manuscript. **Competing interests:** All authors were employees of Genentech Inc., a for-profit institution, when the study was conducted. The authors declare that they have no other competing interests. **Data and materials availability:** The *Il1r1* loxP/loxP mice and the *Grem1*.creERT2 mice were generated at Genentech and are available upon request via a material transfer agreement. All data needed to evaluate the conclusions in the paper are present in the paper or the Supplementary Materials.

Submitted 21 September 2020
Accepted 8 April 2021
Published 7 May 2021
10.1126/sciimmunol.abe8856

Citation: C. B. Cox, E. E. Storm, V. N. Kapoor, J. Chavarria-Smith, D. L. Lin, L. Wang, Y. Li, N. Kljavin, N. Ota, T. W. Bainbridge, K. Anderson, M. Roose-Girma, S. Warming, J. R. Arron, S. J. Turley, F. J. de Sauvage, M. van Lookeren Campagne, IL-1R1–dependent signaling coordinates epithelial regeneration in response to intestinal damage. *Sci. Immunol.* **6**, eabe8856 (2021).

Science Immunology

IL-1R1–dependent signaling coordinates epithelial regeneration in response to intestinal damage

Christian B. Cox, Elaine E. Storm, Varun N. Kapoor, Joseph Chavarria-Smith, David L. Lin, Lifen Wang, Yun Li, Noelyn Kljavin, Naruhisa Ota, Travis W. Bainbridge, Keith Anderson, Merone Roose-Girma, Søren Warming, Joseph R. Arron, Shannon J. Turley, Frederic J. de Sauvage and Menno van Lookeren Campagne

Sci. Immunol. **6**, eabe8856.
DOI: 10.1126/sciimmunol.abe8856

Building back colonic crypts

Restoration of the colonic epithelium after mucosal injury depends on cell renewal initiated by intestinal stem cells (ISCs) and their progeny. Stromal cells near the base of colonic crypts secrete trophic factors for ISCs, but regulation of this process by proinflammatory mediators is not well understood. Cox *et al.* used mouse models of pathogen- or chemical-induced epithelial damage to investigate the contribution of IL-1 and its receptor (IL-1R1) to epithelial restitution. IL-1 release induced GREM1 $^{+}$ mesenchymal cells to produce R-spondin 3, a Wnt agonist supporting ISC renewal and proliferation. IL-1 also promoted innate lymphoid cell production of IL-22, a cytokine supporting colonocyte proliferation. These findings illustrate the need to consider the desirable regenerative properties of IL-1 when designing therapeutic approaches for chronic inflammatory diseases.